Riemann-Lebesgue Forest for Regression

Anonymous authors
Paper under double-blind review

Abstract

We propose a novel ensemble method called Riemann-Lebesgue Forest (RLF) for regression. The core idea in RLF is to mimic the way how a measurable function can be approximated by partitioning its range into a few intervals. With this idea in mind, we develop a new tree learner named Riemann-Lebesgue Tree (RLT) which has a chance to perform Lebesgue type cutting,i.e splitting the node from response Y at certain non-terminal nodes. In other words, we introduce the "splitting type randomness" in our ensemble method. We show that the optimal Lebesgue type cutting results in larger variance reduction in response Y than ordinary CART (Breiman et al., 1984) cutting (an analogue of Riemann partition). Such property is beneficial to the ensemble part of RLF, which is verified by extensive experiments. We also establish the asymptotic normality of RLF under different parameter settings. Two one-dimensional examples are provided to illustrate the flexibility of RLF. The competitive performance of RLF against original random forest (RF)(Breiman, 2001) and boosting methods such as XGboost (Chen & Guestrin, 2016) is demonstrated by experiments in simulation data and real world datasets. Additional experiments further illustrate that RLF could achieve decent performance comparable to that of RF with less running time, especially in large datasets.

1 Introduction

Random Forest (Breiman, 2001) has been a successful ensemble method in regression and classification tasks for decades. Combination of weak decision tree learners reduces the variance of a random forest (RF) and results in a robust improvement in performance. "Feature bagging" further prevents RF from being biased toward strong features which might cause fitted subtrees are correlated. However, the benefit of "feature bagging" may be limited when only small proportion of features are informative. In that case, RF is likely to learn noisy relationship between predictors and response which in the end makes RF underfit the true functional relationship hidden in the data.

Many methods have been proposed to tackle this issue. Heaton (2016) proposed to rule out irrelevant features or perform feature engineering at the beginning of fitting a RF . Another type of ideas is to adjust the way RF selecting informative features. Amaratunga et al. (2008); Ghosh & Cabrera (2021) employed weighted random sampling in choosing the eligible features at each node. Besides the feature weighting method, Xu et al. (2012) used different types of trees such as C4.5, CART, and CHAID to build a hybrid forest. The resulted forest performs well in many high-dimension datasets. Zhou & Feng (2017) employed a sequential multi-grained scanning to discover the feature relationships.

Most of those methods only deal with classification tasks. In this paper, we fill in the gap by proposing a novel forest named Riemann-Lebesgue Forest (RLF) which has superior performance than ordinary Random Forest in regression tasks. The main idea of RLF is to exploit information hidden in the response rather than predictors only. In most types of tree algorithms, people approximate the regression function in the "Riemann" sense. That means the fitted function $\hat{f}(\mathbf{x})$ can be written as follows:

$$\hat{f}(\mathbf{x}) = \sum_{i=1}^{P} \bar{y}_{R_i} \mathbf{1}_{\{\mathbf{x} \in R_i\}} \tag{1}$$

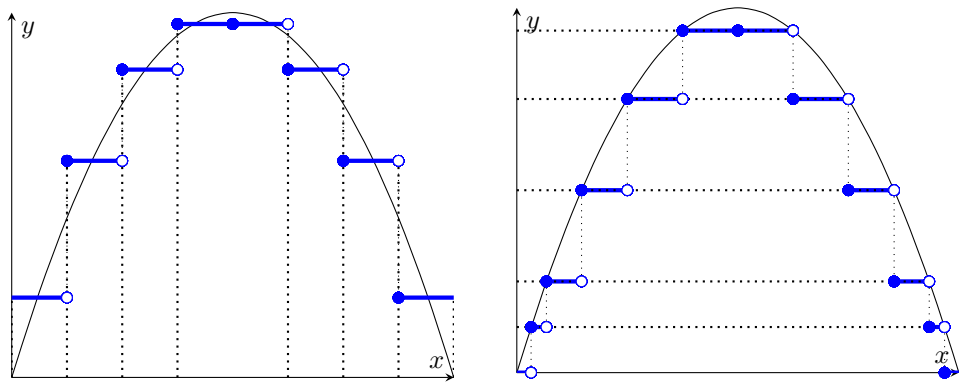

(a) (b)

Figure 1: Two types of function approximation.(a):"Riemann" type approximation. (b): "Lebesgue" type approximation

where each R_i is a hypercube in feature space, $\bar{y}_{R_i}$ represents the mean value of responses lying in the region R_i and P is the total number of hypercubes partitioned. Fig.1(a) gives an example of a smooth function fitted by step functions in one dimension.

As we can see, partitioning x-axis may underfit the true function unless we keep partitioning, which means we take the limit of step functions. Many decision tree algorithms follow this idea by choosing optimal splitting value of optimal feature at each non-terminal node. On the other hand, we know that any measureable function $f : \mathbb{R}^p \to \mathbb{R}$ can be approximated by a sequence of simple functions $\phi_n(\mathbf{x})$, $n = 1, 2, \ldots$. Equation (2) gives an example of simple functions:

$$\phi_n(\mathbf{x}) = \sum_{j=1}^{n2^n} \frac{j-1}{2^n} \chi_{A_{j,n}} + n\chi_{B_n} \tag{2}$$

where $A_{j,n} = f^{-1}([\frac{j-1}{2^n}, \frac{j}{2^n}))$ for $j = 1, 2, ..., n2^n$ and $B_n = f^{-1}([n, \infty])$.

It is now a standard analysis exercise to show that ϕ_n converges to f. Note that if f is finite (which is typically a case in practice), χ_{B_n} will vanish for large n. In other words, we can actually obtain the partitioned feature space indirectly by partitioning the response space (real line) in regression tasks. For comparison, we borrow the term in analysis and name this kind of partition procedure as "Lebesgue" type. Fig. 1(b) gives an example of approximating a function in "Lebesgue" sense. One characteristic for partitioning feature space from response is, the shape of resulted region is not limited to hypercube, which actually enriches the structure of trees in a forest. To overcome the limited structures learned by ordinary RF in sparse models, we incorporate the idea of "Lebesgue" partition in constructing each decision tree. To implement the "Lebesgue" type splitting rule as shown in Fig.1(b) , we can apply the CART-split criterion on response Y which is simple but efficient.

The remaining sections of this paper are organized as following schema. In section 2.1, we illustrate the idea of Riemann-Lebesgue Forest (RLF) in detail. In section 3, we present the potential of Lebesgue cutting in reducing the variance of response Y. Theoretical results such as asymptotic normality of RLF and time complexity analysis are included. We compare the performance of RLF and RF in sparse model and benchmark real datasets in section 4, including the comparisons between GradientBoosting(Trevor Hastie & Friedman, 2009) and XGboosting(Chen & Guestrin, 2016). Simulation results of tuned RLF in models with small signal-to-noise ratio and mixture distribution will be demonstrated as well. Section 5 discusses few characteristics and limitations of RLF and proposes future directions. The R codes for the implementation of RLF, selected real datasets and the simulation results are available in supplementary materials. All simulations and experiments are performed on a laptop with 12th Gen Intel(R) Core(TM) i7-12700H (2.30 GHz) ,16.0 GB RAM and NVIDIA 4070 GPU.

2 Methodology

In section 2.1, we first introduce essential preliminary used in the rest of the paper. We will illustrate how to incorporate "Lebesgue" partition in constructing a CART type tree in section 2.2. Then we apply this new type of tree to the algorithm of Riemann-Lebesgue Forest in section 2.3.

2.1 Preliminary

In this paper, we only consider the regression framework where the data consist of n i.i.d pairs of random variables $Z_i = (\mathbf{X}_i, Y_i) \in \mathcal{X} \times \mathbb{R}, i = 1, 2, ..., n$. Let F_Z be the common distribution of Z_i. WLOG, we can assume the feature space $\mathcal{X} = [0, 1]^d$, where d is the dimension of feature space.

The procedure of generating a Random Forest regression function from Breiman's original algorithm can be summarized as follows:

1. Bootstrapping N times from original dataset.
2. For each bootstrapped dataset, build a CART decision tree based on those subsamples.
3. Take the average of N built trees as the ensemble regressor.

At bootstrapping time i, denote $(X_{i_1}, Y_{i_1}), ..., (X_{i_k}, Y_{i_k})$ be a corresponding subsample of the training set, where k is the subsampling size. If we write the corresponding grown CART tree as $T^{(\omega_i)}((X_{i_1}, Y_{i_1}), ..., (X_{i_k}, Y_{i_k}))$, then the final random forest estimator R_n evaluated at point $\mathbf{x}^*$ can be written as:

$$R_n(\mathbf{x}^*) = \frac{1}{N} \sum_{i=1}^{N} T_{\mathbf{x}^*}^{(\omega_i)}((X_{i_1}, Y_{i_1}), ..., (X_{i_k}, Y_{i_k})) \tag{3}$$

where random variables ω_i represents the randomness from the construction of i-th CART tree. For growing a CART tree, at each node of a tree, the CART-split criterion is applied. m_{try} features will be randomly picked as potential splitting directions. Typically $m_{try} = \lfloor d/3 \rfloor$. On the other hand, the structure of a single CART tree in original forests relies on both predictors and responses in the corresponding subsample, i.e the randomness also comes from resampling (bootstrapping procedure). By assumption in Breiman (2001), $(\omega_i)_{i=1}^N$ are i.i.d and independent of each bootstrapped dataset.

A detailed description of the CART-split criterion is as follows. In CART, a node represents a point in the decision making process of a CART tree. For each CART tree, we have non-terminal node where a split point occurs and a decision is made. Terminal nodes are the nodes only having predicted values and don't have child nodes. Let A be a generic non-terminal node in a decision tree and $N(A)$ be the number of observations lying in node A. A candidate cut is a pair (j, s) where j represents a dimension in $\{1, ..., d\}$ and s is the splitting point along the j-th coordinate of feature space. Since CART-split criterion in RF focuses on splitting predictors, we can view such cutting method as the "Riemann" type splitting rule. Let the set $\mathcal{C}_R = \{(j, s^{(j)}) : j \in \{p_1, ..., p_{m_{try}}\}, s^{(j)} \in \mathbf{X}^{(j)}\}$ consist of all possible cuts in node A and denote $\mathbf{X}_i = (\mathbf{X}_i^{(1)}, ..., \mathbf{X}_i^{(d)})$, where the set $\{p_1, ..., p_{m_{try}}\}$ represents randomly picked feature index in CART, then for any $(j, s) \in \mathcal{C}_R$, the CART-split criterion (Breiman et al., 1984) chooses the optimal (j^*, s^*) such that

$$(j^*, s^*) \in \underset{(j,s) \in \mathcal{C}_R}{\arg\max}\, L(j, s)$$

where

$$L(j, s) = \frac{1}{N(A)} \sum_{i=1}^{n} (Y_i - \bar{Y}_A)^2 \mathbf{1}_{\mathbf{X}_i \in A} - \frac{1}{N(A)} \sum_{i=1}^{n} (Y_i - \bar{Y}_{A_L} \mathbf{1}_{\mathbf{X}_i^{(j)} < s} - \bar{Y}_{A_R} \mathbf{1}_{\mathbf{X}_i^{(j)} \geq z})^2 \mathbf{1}_{\mathbf{X}_i \in A} \tag{4}$$

, $A_L = \{\mathbf{x}_i \in A : \mathbf{x}_i^{(j)} < s, i = 1, 2, ..., n\}$, $A_R = \{\mathbf{x}_i \in A : \mathbf{x}_i^{(j)} \geq s, i = 1, 2, ..., n\}$, $\mathbf{x}_i^{(j)}$ represents the j-th dimension of i-th observation in the given node with size n and $\bar{Y}_A, \bar{Y}_{A_L}, \bar{Y}_{A_R}$ are the averages of responses Y_i with the corresponding features are in sets A, A_L and A_R, respectively.

2.2 Riemann-Lebesgue Tree

To implement the "Lebesgue" type splitting rule as shown in Fig.1(b) , we can apply the CART-split criterion on response Y. Note that we only need to choose the optimal splitting point for Y in this case. Denote $\mathcal{C}_L = \{(j, s) : j \in \{0\}, s \in Y\}$ be the set consist of all possible splitting points for response, then we choose the optimal splitting point s_L^* at node A such that

$$s_L^* \in \arg\max_{s \in \mathcal{C}_L} \tilde{L}(s)$$

where

$$\tilde{L}(s) = \frac{1}{N(A)} \sum_{i=1}^{n} (Y_i - \bar{Y}_A)^2 \mathbf{1}_{Y_i \in A} - \frac{1}{N(A)} \sum_{i=1}^{n} (Y_i - \bar{Y}_{\tilde{A}_D} \mathbf{1}_{Y_i < z} - \bar{Y}_{\tilde{A}_U} \mathbf{1}_{Y_i \geq z})^2 \mathbf{1}_{Y_i \in A} \tag{5}$$

, $\tilde{A}_D = \{\mathbf{x}_i \in A : Y_i < s, i = 1, 2, ..., n\}$, $\tilde{A}_U = \{\mathbf{x}_i \in A : Y_i \geq s, i = 1, 2, ..., n\}$ and $\bar{Y}_A, \bar{Y}_{A_D}, \bar{Y}_{A_U}$ are the averages of responses Y_i with the corresponding features are in sets $A, \tilde{A}_D$ and $\tilde{A}_U$, respectively.

As we can see from equation (4) and equation (5), the "Lebesgue" type splitting rule will go through all potential cutting points for y while the "Riemann" type splitting can only check part of them. We can conclude that $L(j^*, s^*) \leq \tilde{L}(s_L^*)$.

One issue for the "Lebesgue" type splitting rule is overfitting. Suppose the response Y at A' only takes two distinct values, say $Y = 0$ or $Y = 1$, on a node A' . The CART-split criterion for Y can give a perfect split $s_L^* = 0.5$ under some appropriate sets of $\mathcal{C}_L$. In other words, we will have $\tilde{L}(s^*) = \frac{1}{N(A')} \sum_{i=1}^{n} (Y_i - \bar{Y}_{A'})^2 \mathbf{1}_{Y_i \in A'}$. This phenomenon restricts the potential application of "Lebesgue" partitioning in classification task.

To overcome the potential overfitting from the "Lebesgue" type splitting, we apply "Riemann" and "Lebesgue" splitting in a hybrid way. Since we will eventually construct an ensemble learner from Riemann-Lebesgue trees, it's acceptable to introduce a Bernoulli random variable B to determining splitting types at each non-terminal node A. More specifically,

$$B \sim Bernoulli(\tilde{p}), \quad \tilde{p} = \frac{\tilde{L}(s_L^*)}{L(j^*, s^*) + \tilde{L}(s_L^*)}$$

If $B = 1$, the "Riemann" type splitting will be employed, and vice versa. The reason why we define $\tilde{p}$ as above is to control the number of nodes taking "Lebesgue" type splitting. We already seen that $L(j^*, s^*) \leq \tilde{L}(s_L^*)$, so it's expected that there won't be too many "Lebesgue" type nodes and $\tilde{p}$ will play a role of regularization.

Another issue for the Riemann-Lebesgue Tree is the prediction. When there comes a new point $(\mathbf{x}, y)$, we are not allowed to use the information of its response y. That enforces us to estimate the value of response locally when we need to know which partition the new point belongs to.

Linear regression is one of the candidates for the local model. However, it is unstable when the sample size is relatively small. Another choice is the K-Nearest Neighborhood algorithm (KNN). However, the performance of KNN relies on the distance function we used which can be unstable in high-dimensional cases.

In this paper, we choose random forest (with few subtrees) as the local model to obtain an estimate of the response value of a new incoming point since random forest is parameter free and robust for small sample size. When we set the number of subtree be 1, the local random forest reduces to the local decision tree. Experiments in Table S5 implies that local decision tree is good enough in practice. We believe there exists more efficient local models, which is our future work. Algorithm 1 summarizes the procedure of fitting a Riemann-Lebesgue Tree. To our best knowledge, this is the first type of base learner exploring information directly from response.

2.3 Riemann-Lebesgue Forest

Once we establish the way to build a Riemann-Lebesgue Tree, the ensemble version follows immediately. We follow the spirit of original Forest (Breiman, 2001) . That is, growing M trees from different subsamples. Each

Algorithm 1 Riemann-Lebesgue Tree (Fitting)

Require: Training data $\mathcal{D}_n = \{(\mathbf{X}_i, Y_i), i = 1, ..., n\}$. Minimum node size M_{node}. $m_{try} \in \{1, 2, ..., d\}$. Let $N(A)$ denote the number of sample points at node A and A is the root of the tree at the beginning. M_{local} is the number of trees used in local random forests.

1: **if** $N(A) > M_{node}$ **then**
2: Select $M_{try} \subset \{1, 2, ..., d\}$ of cardinality m_{try} without replacement uniformly.
3: Perform CART-split criterion among the selected features, and obtain $j^*, s^*, L(j^*, s^*)$.
4: Perform CART-split criterion with respect to $Y_i \in A$, and obtain $s_L^*, \tilde{L}(s_L^*)$.
5: Calculate $\tilde{p} = \frac{\tilde{L}(s_L^*)}{L(j^*,s^*)+\tilde{L}(s_L^*)}$ and sample $B \sim \text{Bernoulli}(\tilde{p})$.
6: **if** $B = 1$ **then**
7: Cut the node A according to j^*, s^*. Denote A_L and A_R as the two resulting nodes.
8: Repeat steps $1 - 14$ for nodes A_L and A_R.
9: **else**
10: Cut the node A according to s_L^*. Denote A_D and A_U as the two resulting nodes.
11: Fit a random forest model with M_{local} trees w.r.t points in current node A. Call it RF_{local}.
12: Repeat steps $1 - 14$ for nodes A_D and A_U.
13: **else**
14: Set the current node A as a terminal node.
15: **Return:** A collection of nodes and fitted CART-splitting rules

tree is grown as illustrated in Algorithm 1. We employ sampling without replacement (subagging) in ensembling part. The procedure of predicting $\mathbf{x}$ value from a Riemann-Lebesgue Forest (RLF) is described in Algorithm 2. Note that in Algorithm 2, the fitting of local models only relies on subsamples $(X_{i_1}, Y_{i_1}), ..., (X_{i_k}, Y_{i_k})$. Thus we can denote the prediction from i-th RLT as function $H_{\mathbf{x}}^{(\omega_i)}((X_{i_1}, Y_{i_1}), ..., (X_{i_k}, Y_{i_k}))$ where randomness ω_i comes from feature bagging and the random choice of Riemann type cutting and Lebesgue type cutting.

Algorithm 2 Riemann-Lebesgue Forest prediction at $\mathbf{x}$

Require: Original Training data $\mathcal{D}_n = \{(\mathbf{X}_i, Y_i), i = 1, ..., n\}$ with $\mathbf{X}_i \in [0, 1]^d$. Minimum node size M_{node}, $m_{try} \in \{1, 2, ..., d\}$. Number of trees $M > 0$, Number of trees used in local random forests $M_{local} > 0$, $k \in \{1, 2, ..., n\}$ and $\mathbf{x}$.

1: **for** $i = 1$ to M **do**
2: Select k points $(X_{i_1}, Y_{i_1}), ..., (X_{i_k}, Y_{i_k})$ without replacement from $\mathcal{D}_n$.
3: Use selected k points to fit a Riemann-Lebesgue Tree described in Algorithm 1. Hyperparameters such as M_{node}, m_{try} of RLF are shared with each Riemann-Lebesgue Tree.
4: **if** node A is a non-terminal node with Riemann type cutting **then**
5: Suppose the optimal splitting direction is j^* and optimal splitting value at j^* direction is s^*.
6: **if** $\mathbf{x}^{(j)} < s^*$ **then**
7: We send $\mathbf{x}$ to A_L and repeat steps 4-15 until $\mathbf{x}$ arrives at a terminal node
8: **else**
9: We send $\mathbf{x}$ to A_R and repeat steps 4-15 until $\mathbf{x}$ arrives at a terminal node
10: **if** node A is a non-terminal node with Lebesgue type cutting **then**
11: Suppose optimal splitting value of response is s_L^* and the fitted local random forest with M_{local} subtrees is RF_{local}.
12: **if** $RF_{local}(\mathbf{x}) < s_L^*$ **then**
13: We send $\mathbf{x}$ to A_D and repeat steps 4-15 until $\mathbf{x}$ arrives at a terminal node
14: **else**
15: We send $\mathbf{x}$ to A_U and repeat steps 4-15 until $\mathbf{x}$ arrives at a terminal node
16: Denote the averaged values of $Y_i's$ falling in the terminal node of $\mathbf{x}$ as $H_{\mathbf{x}}^{(\omega_i)}((X_{i_1},Y_{i_1}),...,(X_{i_k},Y_{i_k}))$.
17: **Return:** $RLF_M(\mathbf{x}) = \frac{1}{M}\sum_{i=1}^{M} H_{\mathbf{x}}^{(\omega_i)}((X_{i_1}, Y_{i_1}), ..., (X_{i_k}, Y_{i_k}))$, which is the final predicted value of $\mathbf{x}$ from Riemann-Lebesgue Forest.

3 Theoretical analysis of RLF

For the sake of theoretical analysis, we give a theoretical version of Riemann-Lebesgue Forest. Suppose $(Z_1, ..., Z_n)$ are i.i.d from a common underlying distribution F_Z, where $Z_i = (X_i, Y_i)$. Let $h^{(\omega_i)}$ be the random kernel corresponding to the randomness ω_i induced by i-th subsample [1], where $(\omega_i)_{i=1}^n$ are i.i.d with F_ω and independent of each subsample. Denote N as subagging times and k as subagging size. Since we uniformly samples k distinct data points with replacement, the incomplete U-statistic with random kernel (See detailed explanations in Appendix C) at the query point $\mathbf{x}$ is

$$\begin{aligned} U_{n,k,N;\omega}(\mathbf{x}) &= \frac{1}{N}\sum_{i=1}^{N} h^{(\omega(i))}(\mathbf{x}; Z_{i_1}, ..., Z_{i_k}) \\ &= \frac{1}{\binom{n}{k}} \sum_{(n,k)} \frac{W_i}{p} h^{(\omega(i))}(\mathbf{x}; Z_{i_1}, ..., Z_{i_k}) \end{aligned} \tag{6}$$

where $p = N/\binom{n}{k}$ and vector

$$W = (W_1, ..., W_{\binom{n}{k}}) \sim Multinomial(N, \frac{1}{\binom{n}{k}}, ..., \frac{1}{\binom{n}{k}})$$

Note that in asymptotic theory, both N and k can rely on sample size n. We first show Lebesgue cuttings induce smaller L_2 training error than Riemann cutting in section 3.1.In section 3.2, we further give the convergence rate of the asymptotic normality of RLF. To see the time efficiency of RLF in different sizes of data, a complexity analysis is given in section 3.3. Since the Lebesgue part of each Riemann-Lebesgue Tree is essentially splitting the response Y with CART-criterion, many consistency results for traditional RF can be applied to RLF directly. We provide a version of consistency adapted to RLF according to the results of Scornet et al. (2014) in Appendix D.

3.1 Variance reduction of response Y by Lebesgue cuttings

In section 2.2, we conclude that $L(j^*, s^*) \leq \tilde{L}(s_L^*)$ for each partition in constructing a Riemann-Lebesgue Tree. Theorem 3.1 formalizes the above conclusion.

Theorem 3.1. *Let the regression function be $Y = f(\mathbf{X}) + \varepsilon$,where $\mathbf{X} \in \mathbb{R}^d$, $Y \in \mathbb{R}$ and f is a bound measurable function and ε is an independent noise term. Under the procedure defined in equation (4) and equation (5), let $A_1^* = \{Y \geq a^*\}, A_2^* = \{Y < a^*\}$ be the optimal Lebesgue cutting and $B_1^* = \{X^{(j^*)} \geq b^*\}, B_2^* = \{X^{(j^*)} < b^*\}$ be the optimal Riemann(CART) cutting ,then we have:*

$$Var(Y) - Var(Y|A_1^*)P(A_1^*) - Var(Y|A_2^*)P(A_2^*) \geq Var(Y) - Var(Y|B_1^*)P(B_1^*) - Var(Y|B_2^*)P(B_2^*)$$

In other words, the variance reduction of response Y induced by the optimal Lebesgue cutting will be greater or equal to that of optimal Riemann cutting. It follows immediately that a RLT will have smaller L_2 training error than a ordinary CART tree given other tree parameters are the same. According to the bias-variance decomposition, RLF is expected to have smaller mean squared error than RF after the ensembling step. Real-world data experiments in section 4 verify this conjecture. The proof of Theorem 3.1 is based on the variance decomposition formula (law of total variance).

3.2 Convergence rate of the asymptotic normality

Peng et al. (2019) provided sharp Berry-Esseen bounds for of RF under the Bernoulli sampling (Chen & Kato, 2019). The main idea follows from the Stein's method (Chen et al., 2010) and Hoeffding decomposition (Vaart, 2000). Getting inspired by the results in Peng et al. (2019) and Mentch & Hooker (2016), we derive improved Berry-Esseen bounds of RLF for small-N settings (i.e, relatively small number of trees in RLF) where $\lim \frac{n}{N} = \alpha$ and $\alpha > 0$ or ∞ in Theorem 3.2.

[1] More specifically, the randomness of a Riemann-Lebesgue tree given a fixed subsampling comes from the feature bagging and random choice of Riemann type cutting and Lebesgue type cutting.

Theorem 3.2. *Suppose $Z_1, ..., Z_n \overset{i.i.d}{\sim} \mathcal{P}_{\mathbf{Z}}$ and $U_{n,k,N;\omega}$ is defined as in equation (6) with random kernel $h^{(\omega)}(Z_1, ..., Z_k)$. Denote $\theta = \mathbb{E}[h(Z_1, ..., Z_k; \omega)]$. Let $\zeta_k = var(h(Z_1, ..., Z_k; \omega))$, $\zeta_{1,\omega} = \mathbb{E}[g^2(Z_1)]$ where $g(z) = \mathbb{E}[h(z, Z_2, ..., Z_k; \omega)] - \theta$. And $p = N/\binom{n}{k}$. Denote $\alpha_n = \frac{n}{N}$. If $\zeta_k < \infty, \zeta_{1,\omega} > 0, 0 < \eta_0 < 1/2$ and $\mathbb{E}[|h-\theta|^{2m}]/\mathbb{E}^2[|h-\theta|^m]$ is uniformly bounded for $m = 2, 3$, we have the following Berry-Esseen bound for $U_{n,k,N;\omega}$:*

$$
\begin{aligned}
sup_{z\in R}\left|P\left(\frac{\sqrt{N}(U_{n,k,N;\omega}-\theta)}{\sqrt{k^2\zeta_{1,\omega}/\alpha_n+\zeta_k}} \le z\right) - \Phi(z)\right| \le \tilde{C}\Bigg\{ & \frac{\mathbb{E}|g|^3}{n^{1/2}\zeta_{1,\omega}^{3/2}} + \left[\frac{k}{n}\left(\frac{\zeta_k}{k\zeta_{1,\omega}} - 1\right)\right]^{1/2} \\
& + N^{-\frac{1}{2}+\eta_0} + \left(\frac{k}{n}\right)^{1/3} + \frac{\mathbb{E}|h-\theta|^3}{N^{1/2}(\mathbb{E}|h-\theta|^2)^{3/2}} \\
& + \left[\frac{n}{N^{2\eta_0}}\frac{(1-p)\zeta_k}{k^2\zeta_{1,\omega}}\right]^{\frac{1}{2}}\Bigg\}
\end{aligned} \tag{7}
$$

where $\tilde{C}$ is a positive constant and $\Phi(z)$ represents the cumulative distribution function (CDF) for a standard normal distribution.

The proof follows the idea in (Peng et al., 2019) which decomposes the generalized incomplete U-statistic as a sum of complete U-statistic and a remainder. See Appendix G for details. Two asymptotic results can be induced from inequality (7):

1. If $0 < \alpha = \lim \alpha_n < \infty$ and $\frac{n}{N^{2\eta_0}k^2\zeta_{1,\omega}} \to 0$, then $\frac{\sqrt{N}(U_{n,k,N;\omega}-\theta)}{\sqrt{k^2\zeta_{1,\omega}/\alpha+\zeta_k}} \xrightarrow{d} N(0,1)$.
2. If $\lim \alpha_n = \infty$ and $\frac{n}{N^{2\eta_0}k^2\zeta_{1,\omega}} \to 0$, then $\frac{\sqrt{N}(U_{n,k,N;\omega}-\theta)}{\sqrt{\zeta_k}} \xrightarrow{d} N(0,1)$.

where we implicitly assume that $\lim_{n\to\infty}\zeta_k \neq \infty$. More generally, if $k/n \to 0, k^2/n \to \infty$ and $N \to \infty$, the asymptotic normality still holds under some conditions on moments of h. In summary, Theorem 3.2 generalizes the results in Mentch & Hooker (2016); Peng et al. (2019); Ghosal & Hooker (2021) by directly assuming the resampling scheme is sampling without replacement and providing sharp Berry-Esseen bounds for asymptotic normality of RLF. Unlike the bounds in Peng et al. (2019), inequality (7) provides one extra term which comes from the difference between uniformly sampling without replacement and Bernoulli sampling (See Appendix G). It is worth mentioning that the asymptotic results in small-N setting provide a theoretical support for people employing less number of base learners as long as the subsample size k is appropriately designed.

3.3 Complexity analysis

The essential difference between RLF and RF is, a local RF is randomly determined to be fitted at certain nodes of each CART tree. Whether a local RF is fitted relies on a Bernoulli random variable. To analyze the computation time for fitting a RLF, we assume that a local RF will be fit at each non-terminal node of a RLT.

We borrow the notations used in Algorithm 1 and Algorithm 2. In the best case of balanced tree, the time flexibility of building a CART tree is $\mathcal{O}(m_{try} \cdot n \cdot \log_2 n)$ (Trevor Hastie & Friedman, 2009). If the optimal splitting leads to the extreme imbalanced cutting, the worst time flexibility would be $\mathcal{O}(m_{try} \cdot n^2)$ where the tree depth is n.

In the best case of building a Riemann-Lebesgue Tree, we have the following recursion relation

$$T(n) = 2T(\frac{n}{2}) + \mathcal{O}(M_{local} \cdot m_{try} \cdot n \cdot \log_2 n)$$

where $T(\cdot)$ is a measurement of the runtime of a Riemann-Lebesgue Tree. By the limited fourth case in Master theorem (Cormen et al., 2009), $T(n) = \mathcal{O}(M_{local} \cdot m_{try} \cdot n \cdot \log_2^2 n)$. Then the best time complexity of

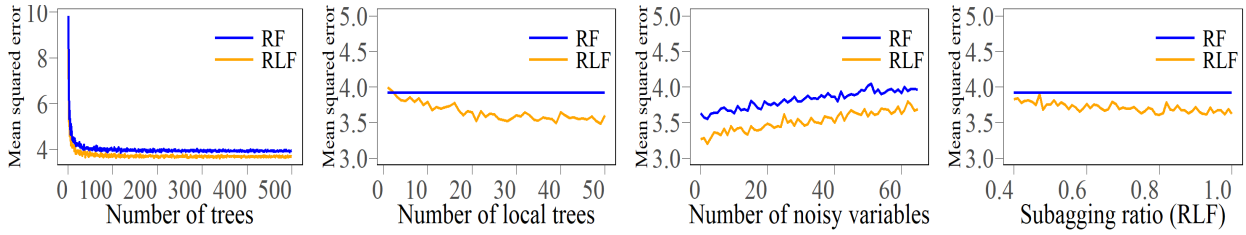

(a) (b) (c) (d)

Figure 2: Test MSEs for RLF and RF. (a) Test MSE as a function of Number of trees, (b) Test MSE rate as a function of Number of local trees, (c) Test MSE as a function of Number of noisy variables, (d) Test MSE as a function of Subagging ratio.

RLF is $\mathcal{O}(M \cdot M_{local} \cdot m_{try} \cdot n \cdot \log_2^2 n)$, which has polylogarithmic runtime. With similar argument, we can see the worst time complexity of RLF is $\mathcal{O}(M \cdot M_{local} \cdot m_{try} \cdot n^2 \cdot \log_2 n)$.

In summary, we observe that the exact difference in complexity in best and worst comes from the factor $M_{local} \cdot \log_2 n$. This implies that the difference of complexity between classical RF and RLF increases when the size of dataset n or the number of local trees M_{local} increases. Table S5 in Appendix E compares the time efficiency and prediction performance of RLF with $M_{local} = 1$ and traditional RF in many datasets. The empirical results show that RLF performs better than RF in general and requires less running time, especially in large datasets. And Table S6 compares the training time of RLF and RF on a simulated dataset with increasing sample size. The results show that the RLF is indeed much more efficient than the RF in large sample size. The possible reason is the efficiency of Lebesgue splitting, which only scans the response instead of screening randomly selected features. In this sense, the scalability of RLF is acceptable than RF. Those observations further supports the superiority of RLF over RF. How to implement RLF in parallelization to speed up training and prediction is one of our future directions.

4 Experiments

4.1 Sparse model

To explore the performance of RLF in sparse model, we consider the following regression model in (Trevor Hastie & Friedman, 2009):

$$Y = 10 \cdot \prod_{j=1}^{5} e^{-2X_j^2} + \sum_{j=6}^{35} X_j + \varepsilon, \quad \varepsilon \sim N(0, \sigma^2)$$

where $\mathbf{X}_j$ is the j-th dimension of an observation $\mathbf{X}$. The response $\mathbf{Y} \in \mathbb{R}$ and random sample X will be i.i.d and uniformly distributed on the 100-dimension unit cube $[0, 1]^{100}$. In this case, the effective dimension is 35. And σ is set to be 1.3 so that the signal-to-noise ratio is approximately 2. Fig. 2 summarizes testing MSEs for RLF and RF as functions of different hyperparameters. As we can see, given data-driven $\tilde{p}$, RLF outperforms RF in almost all settings. See detailed experiment settings and analysis in Appendix B.

4.2 Real Data Performance

We used 10-folds stratified cross-validation [2] to compare the performance of RLF and RF on 30 benchmark real datasets from Fischer et al. (2023). The size of datasets ranges from five hundred to nearly fifty thousand observations. For time efficiency and consistency, we set the number of trees in RLF and RF to be 100 and subtrees in local RF in Lebesgue part of RLF to be 10, i.e M_{local}=10. See Appendix A for the detail of datasets and statistical significance tests employed.

[2]That means stratified sampling method was employed to ensure the distribution of response is the same across the training and testing sets

We observe that RLF reaches roughly the same mean-squared-error as RF for most datasets and outperforms RF in 20 datasets where eight of them are statistically significant. The binomial test for win/loss ratio of RLF also shows that RLF does better job than RF statistically.

Table 1: Mean squared error and corresponding 95% margin of error (based on 10-folds cross-validation) for Riemann–Lebesgue Forest(100,10) vs.Random Forest(100)

Dataset	RLF(100,10)	RF(100)	Dataset	RLF(100,10)	RF(100)
FF	**4205.21 ±5612.77**	4303.31±5432.01	CPU	**5.72±0.63**	5.92±0.59
SP	1.90±0.87	**1.88±0.82**	KRA	**0.0188 ±0.00062***	0.0214 ±0.00059
EE	**1.258±0.32**	1.262±0.35	PUMA	**4.97e-4 ±1.38e-5***	5.14e-4±1.67e-5
CAR	**5374313 ±787019.9**	5390741 ±840508.3	GS	**1.2e-4 ±4.06e-6***	1.5e-4±4.71e-6
QSAR	**0.7568±0.14**	0.7594±0.13	BH	**0.01 ±0.01**	0.011±0.012
CCS	28.34±4.87	**28.19 ±4.09**	NPP	**5.97e-7±6.84e-8**	6.5e-7±9.10e-8
SOC	587.87±205.53	**565.08 ±204.29**	MH	**0.02±0.00093***	0.022 ±0.0011
GOM	**240.67±38.74**	247.61±39.16	FIFA	**0.5775±0.026**	0.5796±0.024
SF	**0.66±0.21**	0.67 ±0.2	KC	0.041±0.0013	**0.037±0.0013***
ASN	**11.87 ±1.28***	13.02±1.30	SUC	83.16±2.26	**82.38±2.27**
WINER	0.3319±0.034	**0.3299 ±0.035**	CH	**0.056±0.0026***	0.059±0.0026
AUV	**8073182±1513348***	9368024±833367.9	HI	217.64±4.91	**212.12±4.42***
SG	0.01367±0.0045	**0.01364±0.0046**	CPS	**0.2766±0.0077**	0.2772±0.0068
ABA	4.63 ±0.54	**4.58±0.56**	PP	**11.94±0.16***	12.09±0.13
WINEW	0.3670±0.021	**0.3612±0.022**	SA	**6.13±0.16**	6.26±0.21

The better performing values are highlighted in bold and significant results are marked with "".

4.3 Tuning of Splitting control probability $\tilde{p}$

Instead of using data-driven $\tilde{p}$, we can set the control probability $\tilde{p}$ as a tunable parameter when constructing a RLT. That is to say, we set $\tilde{p}$ be a fixed value for all nodes in a RLT. For instance, under the same sparse model defined in section 4.1, Fig.3(a) indicates that the sparse model favors more Lebesgue cuttings.[3] This is consistent with the intuition that noisy variables weaken the effectiveness of Riemann cutting. In this section, we provide two one-dimensional examples to illustrate the flexibility of RLF with tuned $\tilde{p}$. One is designed to have small signal-to-noise ratio. The other is a mixture model with prior probability where we anticipate that RLF will perform better because of nature the Lebesgue type cutting. Test MSEs of RLF as functions of $\tilde{p}$ in Fig S4(a) and S4(b) exhibit the potential benefit of tuning control probability $\tilde{p}$. See details of tuning procedure in Appendix H.

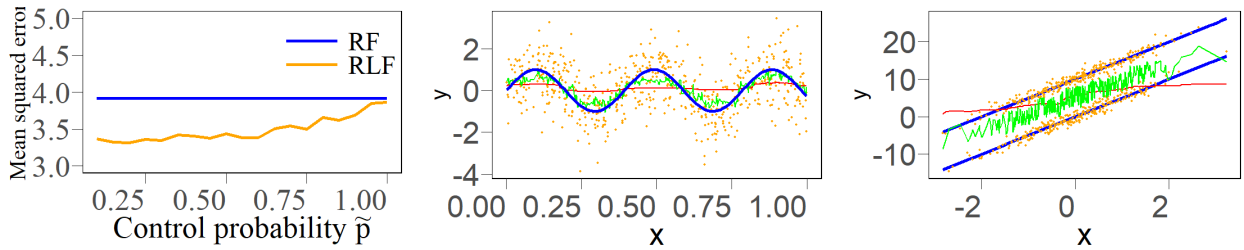

(a) Sparse model (b) Example 1 (c) Example 2

Figure 3: (a) Test MSEs for RLF and RF as functions of control probability $\tilde{p}$. Orange points in (b) and (c) represent test samples generated by two models. Blue solid lines are the underlying functions; Green lines are the predicted curves for optimal RLFs while the red lines are the predicted curve of optimal RF in two examples.

[3]Since RF doesn't have parameter $\tilde{p}$ so the Test MSE curve of RF is a constant function w.r.t $\tilde{p}$

Example 1: Small signal-to-noise ratio

Figure 3(b) demonstrates the predicted regression curves from tuned RLF and tuned RF in one-dimensional case. Our synthetic model is based on the sine function used in Cai et al. (2023):

$$Y = \sin(16X) + \varepsilon, \quad \varepsilon \sim N(0, \sigma^2)$$

where $X \sim \text{Unif}[0, 1]$ and $\sigma = 1$. Predicted curves in Fig.3(b) show that tuned RLF is robust to relative high level of noise and it is capable to identify the pattern in response while traditional RF is too conservative in this case. Table S7 in Appendix H lists validation MSE of top 10 models with tuning parameters for RF and RLF. Based on the top 10 models, we can see RLF generally outperforms RF in this case. Indeed, the testing MSE under best RF is 1.283 while the testing MSE of best RLF is 1.018 (See Table S8 in Appendix H). Another interesting phenomenon is , when the noise level is high, RLF prefers using more Riemann type cuttings to achieve better performance as top 5 tuned RLFs in Table S8 have relatively large value of $\tilde{p}$.

Example 2: Mixture model with prior probability

In second example, we consider a mixture model as follows:

$$Y = \begin{cases} 5X + \varepsilon & \text{if} \quad C = 1 \\ 10 + 5X + \varepsilon & \text{if} \quad C = 2 \end{cases} \tag{8}$$

where $X, \varepsilon \overset{i.i.d}{\sim} N(0, 1)$ and the random variable C is uniformly distributed on $\{1, 2\}$. To generate an observation of response, we first randomly pick a value of state variable C from $\{1, 2\}$ and generate Y according to the model defined in equation (8). In this way, Y will follow a mixture Gaussian distribution. Figure 3(c) illustrates that RLF is capable of capturing the complicated distribution of response with the help of Lebesgue cuttings, while traditional RF fails in detecting the complex pattern in response.

Similarly, Table S9 in Appendix H lists validation MSEs of top 10 models with tuning parameters and the testing error of best RLF (29.87) is smaller than that of best RF (35.17) showing that RLF also beats RF in this case. It is worth mentioning that Table S9 gives us a clue that when response Y has mixture distribution, RLF favors more Lebesgue cuttings since top 5 tuned RLF models tend to employ relatively small value of $\tilde{p}$.

4.4 Extra experiments of RLF with tuned $\tilde{p}$

We perform extra experiments on 26 datasets listed in Table 1 to show the strength of RLF after parameter tuning. Four large datasets are excluded due to the time efficiency of parameter tuning. Table 2 shows that tuned RLF still outperforms tuned RF in many real world datasets and wins more often than in original experiments. More specifically, tuned RLF wins in 23 datasets among which 12 of them are statistically significant. See Appendix I for detailed settings for tuning process.

Table 2: Averaged MSEs and 95% marginal errors for Best RLF and Best RF

Dataset	Best RLF	Best RF	Dataset	Best RLF	Best RF
FF	**4221.49 ±9191.91**	4376.29±8922.14	ABA	4.66±0.39	**4.63±0.38**
SP	**1.78 ±0.78**	1.98±0.73	WINEW	**0.398±0.025**	0.403±0.0264
EE	**0.54 ±0.29***	1.50±0.35	CPU	**5.67±0.58***	6.15±0.43
CAR	**5194266 ±1287865**	5622327±1482889	KRA	**0.019±0.0008***	0.024±0.0013
QSAR	**0.79 ±0.10**	0.80±0.13	PUMA	**0.00048±1.35e-05***	0.00053±1.82e-05
CCS	**27.11 ±3.52***	37.23±7.0	GS	**0.00011±7.95e-06***	0.00016±8.07e-06
SOC	**405.63±376.21**	621.75±528.39	BH	**0.0061±0.0032**	0.0069±0.0040
GOM	**255.49±56.60**	263.16±64.10	NPP	**7.79e-07±1.96e-07***	1.08e-06±1.95e-07
SF	0.67±0.19	**0.62±0.21**	MH	**0.021±0.0017***	0.023±0.0012
ASN	**5.67±1.07***	14.14±2.00	FIFA	**0.578±0.011**	0.581±0.010
WINER	**0.347±0.026**	0.349±0.026	SUC	**89.67±11.40**	91.80±10.36
AUV	**4192163±1236743***	9878887±1670280	CH	**0.056±0.018***	0.062±0.019
SG	**0.0137±0.0049***	0.0143±0.0049	CPS	0.279±0.0061	**0.27±0.0060**

The better performing values are highlighted in bold and significant results are marked with "*".

4.5 Comparison with Boosting methods

To see the potential of RLF among various tree-based models, we conducted experiments comparing the testing MSE(10-folds cross-validaiton) of RLF, GradientBoosting(GB)(Trevor Hastie & Friedman, 2009) and XGboost(Chen & Guestrin, 2016). The number of base tress in GB and XGboost are 1000 and the subagging ratio is 0.8. Other parameters are set by default. The number of RLTs is 100 in RLF and $M_{local} = 10$ for local RFs in RLF. The control probability $\tilde{p} = 0.8$. Table 3 shows that RLF is comparable to XGboost in general and RLF outperforms GradientBoosting in most cases. The competitive performance of RLF in large datasets further illustrates the potential of RLF.

Table 3: Testing MSEs and 95% marginal error for RLF, GB and XGboost

Dataset	#Observations	#Features	RLF(100,10,0.8)	GB(1000,0.8)	XGboost(1000,0.8)
FF	517	11	**4293±5527.51**	4694.78±5363.52	6624.42±5518.72
SP	649	31	**1.76±0.79**	2.13±0.90	2.27±0.90
EE	768	9	0.74±0.27	1.09±0.22	0.09±0.03
CAR	804	18	**4916065±776998.4**	8781409±1181857	5802233±988893.7
QSAR	908	7	**0.75±0.13**	0.85±0.13	0.97±0.17
CCS	1030	9	23.73±4.28	28.87±3.68	**20.05±8.49**
SOC	1056	6	422.94±164.72	460.71±135.03	**325.54±167.66**
GOM	1059	117	**240.13±28.46**	266.72±37.29	269.68±24.96
SF	1066	11	0.71±0.20	**0.61±0.19**	0.95±0.18
ASN	1503	6	6.95±0.79	20.94±2.25	**1.58±0.39**
WINER	1599	12	**0.32±0.13**	0.41±0.038	0.38±0.04
AUV	2043	8	4324542±711281.7	27726483±1730233	**155060.7±38776.38**
SG	3107	7	0.013±0.005	0.016±0.005	**0.012±0.003**
ABA	4177	9	**4.6±0.58**	4.79±0.43	5.76±0.65
WINEW	4898	12	**0.36±0.02**	0.50±0.03	0.4±0.02
CPU	8192	22	**5.45±0.49**	6.25±0.47	6.00±1.45
KRA	8192	9	0.017±0.0008	0.04±0.0008	**0.016±0.0007**
PUMA	8192	33	**0.00047±0.0008**	0.00112±0.0008	0.00056±0.0007
GS	10000	13	0.00011±3.81e-6	0.0003±9.69e-6	**8.97e-5±2.42e-6**
BH	10692	10	0.01±0.01	0.014±0.008	**0.004±0.006**
NPP	11934	15	**4.81e-7±5.12e-8**	3.9e-5±1.44e-6	8.67e-7±8.11e-8
MH	13932	16	**0.02±0.0009**	0.032±0.0017	0.023±0.001
FIFA	19178	29	**0.57±0.026**	0.60±0.025	0.61±0.027
SUC	20263	82	**82.18±6.60**	286.6±8.78	94.10±5.62
CH	20460	9	0.053±0.0026	0.13±0.003	**0.052±0.0027**
KC	21613	22	0.036±0.0012	0.055±0.0015	**0.028±0.0001**
HI	22272	12	226.82±4.39	220.68±3.68	**220.42±5.12**
CPS	28155	7	**0.277±0.004**	0.282±0.0047	0.283±0.0054
PP	45730	10	**11.59±0.21**	28.60±0.32	15.12±0.25
SA	48933	22	**5.34±0.074**	68.55±2.47	7.72±0.23

The best performing values are highlighted in bold.

4.6 Ablation study with feature selection

To see how much gain comes from using response Y to guide splits instead of filtering noisy features, we conducted extra comparisons between RLF and two-stage RF where we first do a feature selection to remove most noisy features and then fit a RF. In the feature selection part, we follows the strategy of taking the top 30% important features based on variable importance score from a fitted RF. The other training details follow Appendix E for the sake of time efficiency. The results summarized in Table S11 in Appendix J illustrates that the original RLF still outperforms RF(with feature selection) in most real datasets and if we apply the same feature selection method to RLF, the performance of RLF will be better than that of RF as well, which another strong evidence of the superiority of RLF.

What's more, in sparse model example (section 4.1), we took the top 35 most important features through variable importance score. The 10-fold cross-validation testing MSE of RLF is less than that of RF with feature selection which strengthens the advantage of RLF. See Table S12 in Appendix J

5 Discussion and Limitation

Theorem 3.1 has shown the benefit of Lebesgue cutting in reducing the L_2 error of RLF. Section 4.3 further demonstrates the flexibility of RLF in many complicated models and real world datasets with tuned $\tilde{p}$. The asymptotic normality in section 3 is useful for statistical inference such as confidence intervals and hypothesis testings (Mentch & Hooker, 2016). It's possible to obtain a Berry-Esseen bound of RLF in large N-setting by similar arguments. However, this bound can be worthless in practice as it's requires $N \gg n$ and we decide not to pursue it in this paper.

Although the experiment results show that tuned $\tilde{p}$ is superior than data-driven $\tilde{p}$, the cross-validation tuning process is less time efficient than data-driven methods in large datasets. How to choose the optimal value of $\tilde{p}$ is an interesting problem. On the other hand, we employ a Bernoulli random variable to determine the splitting type at each non-terminal node. It's possible that there are other better regularization methods to control the overfitting resulted from Lebesgue splitting. Connecting RLT with boosting would be another riveting direction as RLT is essentially a new kind of base learner in ensemble methods.

Developing a more efficient local model for RLF would benefit RLF in large datasets. As we discussed in section 3.3, the time efficiency of current RLF can be improved by employing less number of subtrees in local forest and setting larger value of control probability $\tilde{p}$ so that each RLT won't perform too many Lebesgue splittings. For example, if we set $M_{local} = 1$, that is, we employ a local decision tree as the local model in RLF, the results in Table S5 still demonstrate that RLF could achieve comparable testing MSEs with less running time, especially in large datasets, which validates the superiority of RLF over RF.

Readers may view the use of Riemann-Lebesgue Tree as counterintuitive if the local models (e.g local forests or local decision tree) can estimate response Y accurately. However, the local models don't have to be as good as the RLF or RLT since we only require the local models to indicate the direction, not the precise prediction of new points. What's more, when the response is complicated, as indicated in example 2 (mixture model with prior probability), we can employ more Lebesgue type splittings in RLF to partition the range of response Y. As a result, the local distribution of Y becomes simpler which will relax the requirement of the precision of local models. The flexibility of RLF comes from the control probability $\tilde{p}$, which controls the number of Lebesgue type splittings in each RLT and can be tailored to different cases.

In more general scenarios, how to cope with possible missing values deserves deep inspection since RLF replies heavily on the information from all variables and it's possible that the prediction of local RF in RLF could be misled by missing values. Actually, in practice, we can perform imputation by rough average/mode, or by an averaging/mode based on proximities during the data preprocessing. Table S13 in Appendix K illustrates the promising performance of RLF with simple median imputation strategy in two real datasets with missing values as described in Fischer et al. (2023). How to further generalize the implementation of RLF in missing value cases is one of our future work and is out of the scope of our current paper.

Broader Impact Statement

In summary, this paper aims to provide new ideas in designing base tree learners. We analyze few theoretical properties of RLF. which should have no societal impacts. As to the application of RLF in regression tasks, we think most possible impacts may come from the ethics of datasets. It's possible that some public datasets be biased during data collection process. For example, information from minority may be inappropriately ignored or processed. In this sense, users should be careful in selecting datasets. In our paper, all datasets used in experiments are available on openml (Fischer et al., 2023)

References

Dhammika Amaratunga, Javier Cabrera, and Yung-Seop Lee. Enriched random forests. *Bioinformatics*, 24 (18):2010–2014, 07 2008. ISSN 1367-4803. doi:10.1093/bioinformatics/btn356. URL `https://doi.org/10.1093/bioinformatics/btn356`.

L. Breiman. Random forests. *Machine Learning*, 45:5–32, 2001. URL https://api.semanticscholar.org/CorpusID:89141.

L. Breiman, Jerome H. Friedman, Richard A. Olshen, and C. J. Stone. Classification and regression trees. 1984.

Yuchao Cai, Yuheng Ma, Yiwei Dong, and Hanfang Yang. Extrapolated random tree for regression. In Andreas Krause, Emma Brunskill, Kyunghyun Cho, Barbara Engelhardt, Sivan Sabato, and Jonathan Scarlett (eds.), *Proceedings of the 40th International Conference on Machine Learning*, volume 202 of *Proceedings of Machine Learning Research*, pp. 3442–3468. PMLR, 23–29 Jul 2023. URL https://proceedings.mlr.press/v202/cai23d.html.

Louis H. Y. Chen, Larry Goldstein, and Qi-Man Shao. Normal approximation by stein's method. 2010. URL https://api.semanticscholar.org/CorpusID:118531844.

Tianqi Chen and Carlos Guestrin. Xgboost: A scalable tree boosting system. In *Proceedings of the 22nd ACM SIGKDD International Conference on Knowledge Discovery and Data Mining*, KDD '16, pp. 785–794, New York, NY, USA, 2016. Association for Computing Machinery. ISBN 9781450342322. doi:10.1145/2939672.2939785. URL https://doi.org/10.1145/2939672.2939785.

Xiaohui Chen and Kengo Kato. Randomized incomplete u-statistics in high dimensions. *The Annals of Statistics*, 47(6):pp. 3127–3156, 2019. ISSN 00905364, 21688966. URL https://www.jstor.org/stable/26867161.

Thomas H. Cormen, Charles E. Leiserson, Ronald L. Rivest, and Clifford Stein. *Introduction to Algorithms, Third Edition*. The MIT Press, 3rd edition, 2009. ISBN 0262033844.

Bradley Efron and Robert Tibshirani. Improvements on cross-validation: The .632+ bootstrap method. *Journal of the American Statistical Association*, 92(438):548–560, 1997. ISSN 01621459. URL http://www.jstor.org/stable/2965703.

Sebastian Felix Fischer, Liana Harutyunyan Matthias Feurer, and Bernd Bischl. OpenML-CTR23 – a curated tabular regression benchmarking suite. In *AutoML Conference 2023 (Workshop)*, 2023. URL https://openreview.net/forum?id=HebAOoMm94.

Indrayudh Ghosal and Giles Hooker. Boosting random forests to reduce bias; one-step boosted forest and its variance estimate. *Journal of Computational and Graphical Statistics*, 30(2):493–502, 2021. doi:10.1080/10618600.2020.1820345. URL https://doi.org/10.1080/10618600.2020.1820345.

Debopriya Ghosh and Javier Cabrera. Enriched random forest for high dimensional genomic data. *IEEE/ACM Trans. Comput. Biol. Bioinformatics*, 19(5):2817–2828, jun 2021. ISSN 1545-5963. doi:10.1109/TCBB.2021.3089417. URL https://doi.org/10.1109/TCBB.2021.3089417.

Jeff Heaton. An empirical analysis of feature engineering for predictive modeling. In *SoutheastCon 2016*, pp. 1–6, 2016. doi:10.1109/SECON.2016.7506650.

Niels Landwehr, Mark A. Hall, and Eibe Frank. Logistic model trees. *Machine Learning*, 59:161–205, 2003. URL https://api.semanticscholar.org/CorpusID:6306536.

Alan J. Lee. U-statistics: Theory and practice. 1990. URL https://api.semanticscholar.org/CorpusID:125216198.

Lucas Mentch and Giles Hooker. Quantifying uncertainty in random forests via confidence intervals and hypothesis tests. *J. Mach. Learn. Res.*, 17(1):841–881, jan 2016. ISSN 1532-4435.

Claude Nadeau and Y. Bengio. Inference for the generalization error. *Machine Learning*, 52:239–281, 01 2003. doi:10.1023/A:1024068626366.

Weiguang Peng, Tim Coleman, and Lucas K. Mentch. Rates of convergence for random forests via generalized u-statistics. *Electronic Journal of Statistics*, 2019. URL https://api.semanticscholar.org/CorpusID:209942194.

Erwan Scornet, Gérard Biau, and Jean-Philippe Vert. Consistency of random forests. *Annals of Statistics*, 43: 1716–1741, 2014. URL https://api.semanticscholar.org/CorpusID:8869713.

Robert Tibshirani Trevor Hastie and Jerome Friedman. *The Elements of Statistical Learning*. Springer New York, 2009. ISBN 9780387848587. doi:10.1007/b94608. URL http://dx.doi.org/10.1007/b94608.

A. W. van der Vaart. *Asymptotic Statistics*. Number 9780521784504 in Cambridge Books. Cambridge University Press, July 2000. URL https://ideas.repec.org/b/cup/cbooks/9780521784504.html.

Baoxun Xu, Joshua Zhexue Huang, Graham J. Williams, and Yunming Ye. Hybrid weighted random forests for classifying very high-dimensional data. 2012. URL https://api.semanticscholar.org/CorpusID:10700381.

Zhi-Hua Zhou and Ji Feng. Deep forest: Towards an alternative to deep neural networks. In *Proceedings of the Twenty-Sixth International Joint Conference on Artificial Intelligence, IJCAI-17*, pp. 3553–3559, 2017. doi:10.24963/ijcai.2017/497. URL https://doi.org/10.24963/ijcai.2017/497.

Appendix

A Data preparation and statistic tools used in real data experiments

Table S4 summarizes the datasets we used in experiments. Note that there are 35 datasets in original benchmarks. We didn't perform comparison on the datasets with the number of instances more than 50,000 since the complexity of RLF is relatively higher than RF. We also excluded datasets with missing values whose results might be unfair. We took logarithm transformation for some datasets to alleviate the impact of skewness. As described in Algorithm 2, we set the subagging ratio to be 0.632, which should have the same efficiency with bootstrapping (Efron & Tibshirani, 1997)

Table S4 : Real datasets used for the experiments,sorted by size

Dataset	Observations	Numerical features	Symbolic features	Log transformation
Forestfire (FF)	517	9	2	No
Student performance (SP)	649	14	17	No
Energy efficiency (EE)	768	9	0	No
Cars(CAR)	804	18	0	No
QSAR fish toxicity (QSAR)	908	7	0	No
Concrete Compressive Strength (CCS)	1030	9	0	No
Socmob(SOC)	1056	2	4	No
Geographical Origin Of Music (GOM)	1059	117	0	No
Solar Flare (SF)	1066	3	8	No
Airfoil Self-Noise (ASN)	1503	6	0	No
Red wine quality (WINER)	1599	12	0	No
Auction Verification (AUV)	2043	7	1	No
Space Ga (SG)	3107	7	0	No
Abalone (ABA)	4177	8	1	No
Winequality-white (WINEW)	4898	12	0	No
CPU Activity (CPU)	8192	22	0	No
Kinematics of Robot Arm (KRA)	8192	9	0	No
Pumadyn32nh (PUMA)	8192	33	0	No
Grid Stability (GS)	10000	13	0	No
Brazil Housing (BH)	10692	6	4	Yes
Naval propulsion plant (NPP)	11934	15	0	No
Miami housing (MH)	13932	16	0	Yes
Fifa (FIFA)	19178	28	1	Yes
Kings county (KC)	21613	18	4	Yes
Superconductivity (SUC)	20263	82	0	No
Califonia housing (CH)	20460	9	0	Yes
Health insurance (HI)	22272	5	7	No
Cps88wages (CPS)	28155	3	4	Yes
Physiochemical Protein (PP)	45730	10	0	No
Sarcos (SA)	48933	22	0	No

We employed a corrected resampled t-test (Nadeau & Bengio, 2003; Landwehr et al., 2003), to identify whether one method significantly outperforms another at 5% significance level. This test rectifies the dependencies of results induced by overlapped data points and has correct size and good power. The corresponding statistic is

$$t = \frac{\frac{1}{V}\sum_{t=1}^{V} r_t}{\sqrt{(\frac{1}{V} + \frac{n_2}{n_1})\hat{\sigma}^2}}$$

where V is the number of validation experiments performed (ten in our case), r_t is the difference in MSE between RLF and RF on t-th fold. $\hat{\sigma}$ is the sample standard deviation of differences. n_1 is the number ofdata points used for training and $n_2$is the number of testing cases. In our case, $n_2/n_1 = 1/9$ since we used 10-folds cross-validation.

B Experiment details in sparse model

There are 1000 training cases and 500 test observations. Each subplot in Figure 2 illustrates the curves of mean squared error for RLF and RF, as functions of a single hyperparameter. The default setting for RLF is $M = 100, M_{local} = 10, \alpha = 0.632, M_{node} = 5$. Same setting except M_{local} applies to RF. To obtain, for example the test MSE as a function of number of global trees, we set $M = 1, 2, ..., 500$ while other parameters remain the same with default setting. Similar strategy was applied to the other three hyperparameters we are interested.

In Fig.2(a) , we let RLF and RF share the same the number of trees. We observe that the test MSE for RLF decreases more than that of RF as the number of trees increases. In Fig.2(b) , RF is fitted under default setting while we only changed the number of local trees used in local random forest of RLF. As we can see, large number of local trees indeed benefits the performance of RLF. On the other hand, in order to control the computation time burden, the number of local trees should not be too large. Fig.2(c) implies that increasing the number of noisy variables in the regression model will impair both the performance of RLF and RF. Nevertheless, RLF always outperforms RF, which is anticipated. To see the impact of subagging ratio on RLF, we first controlled the result from ordinary RF under default setting and increased subagging ratio, which determines the subsample size in RLF, from 0.4 to 1. The test MSE curve for RLF in Fig.2(d) indicates that even a small subagging ratio could generatea decent result. We can therefore set the subagging ratio relatively small to make RLF efficient.

C Incomplete U-statistics

Before give the definition of incomplete U-statistics, we first give a brief introduction of U-statistics. We borrow notations from (Vaart, 2000). Suppose we have i.i.d samples $X_1, ..., X_n$ from an unknown distribution, and we want to estimate a parameter θ defined as follows

$$\theta = \mathbb{E}h(X_1, ..., X_r)$$

where the function h is permutation symmetric in its r arguments and we call h as a kernel function with order r. Then a U-statistic with kernel h is defined as

$$U = \frac{1}{\binom{n}{r}} \sum_{\beta} h(X_{\beta_1}, ..., X_{\beta_r})$$

where the sum is taken over all all unordered subsets β with r distinct elements from $\{1, ..., n\}$.

Note that the U-statistic is an unbiased estimator for θ and has smaller variance than a single kernel h. In practice, it's unrealistic to average all $\binom{n}{r}$ kernels (trees). To make U-statistics more useful in applications, we can define an incomplete U-statistic which utilizes smaller number of subsets as follows:

$$U_{n,r,N} = \frac{1}{N} \sum_{i=1}^{N} h(X_{\beta_1,...,X_{\beta_r}})$$

when $N = \binom{n}{r}$, we obtain a complete U-statistic.

When the total number of subsamples of size r taken from a sample of size n is large, it may be convenient to use instead an 'incomplete' U-statistic based on N suitably selected subsamples. Asymptotically, it can be shown that an incomplete U-statistic may be asymptotically efficient compared with the 'complete' one even when N increases much less rapidly than the total number. See more explanations and applications for complete/incomplete U-statistics in (Vaart, 2000; Lee, 1990; Peng et al., 2019; Chen et al., 2010). In a Riemann-Lebesgue Forest, each tree can be viewed as a random kernel since it is permutation symmetric w.r.t inputs. The randomness of the kernel comes from feature bagging and subsampling and cutting types. Similar definition can be applied to RF as well.

D Consistency of RLF

Based on the results from (Scornet et al., 2014), it's relatively easy to derive the consistency of RLF under an additive regression model as follows:

$$Y = \sum_{j=1}^{p} m_j(\mathbf{X}_j) + \varepsilon \tag{9}$$

where $\mathbf{X} = (\mathbf{X}_1, .., \mathbf{X}_p)$ is uniformly distributed over $[0,1]^p$, the noise $\varepsilon \sim N(0, \sigma^2)$ has finite variance and is independent of $\mathbf{X}$. Each component function m_j is continuous.

When there are only $S(< p)$ effective dimensions of the model, the sparse version of equation 9 becomes

$$Y = \sum_{j=1}^{S} m_j(\mathbf{X}_j) + \varepsilon$$

which is exactly the condition where RLF may perform better. Therefore the additive regression model is a good framework for studying the consistency of RLF. Since the Lebesgue part of each Riemann-Lebesgue Tree is essentially splitting the response Y with CART-criterion, many consistency results for CART can be applied to RLT directly.

For example,Breiman et al. (1984) proved the consistency of CART under the assumptions of shrinking diameter of cell partition and lower bounds of empirical distribution of X. Scornet et al. (2014) shown the consistency of RF under the assumption of additive regression model and appropriate complexity of the tree partition.

We now state one version of consistency adapted to RLF where we assume that the total number of nodes t_n in each RLT approaches to infinity more slowly than the subsample size k_n. The proof follows immediately from the argument for Theorem 1 in (Scornet et al., 2014).

Theorem D.1. *Assume the response Y is generated from the sparse model defined in equation 9. Then, given $k_n \to \infty, t_n \to \infty$ and $t_n(logk_n)^9/k_n \to 0$ where k_n is the subagging size and t_n is the number of terminal nodes in each Riemann-Lebesgue Tree, we have*

$$\lim_{n\to\infty} \mathbb{E}_X[h^*_{n,k,N}(\mathbf{X}) - m(\mathbf{X})]^2 = 0$$

where $m(\mathbf{X}) = \mathbb{E}[Y|X]$, $h^*_{n,k,N}(\mathbf{X}) = \mathbb{E}_{\omega,Z}[h^{(\omega)}(X;Z)]$. The consistency of empirical averaged RLF estimate follows from the law of large numbers.

Note that Theorem D.1 still holds even when we select all data points for each tree, which means controlling the number of nodes t_n via minimal size of nodes M_{node} is sufficient for the error bound of RLF. According to (Scornet et al., 2014), the term $(\log k_n)^9$ results from the assumption of Gaussian noise. We can replace it by a bounded random variable so that the term $(\log k_n)^9$ becomes $logk_n$, which can be regarded as the complexity of a single RLT partition,

E Running time for RLF and RF

For completeness, Table S5 compares averaged running time (in seconds) and margin of error with 95% confidence level of RLF,RF on our selected datasets in manuscript. For RLF, $M = 100, M_{local} = 1$ and $\tilde{p} = 0.8$. For RF, $M = 100$. Other parameters are set by default values. We ran 10-fold cross-validation. We calculated the running time as sum of training time and prediction time.

Table S5 : Average running time (in seconds) and Testing MSE for RLF(100,1),RF(100)

Dataset	Observations	# Features	RLF(s)	RF(s)	RLF(Testing MSE)	RF(Testing MSE)
FF	517	11	0.11±0.005	**0.094± 0.028**	**4206.94 ± 5398.57**	4434.81 ± 5463.97
SP	649	31	0.20±0.028	**0.19±0.004**	1.78±0.78	1.78±0.75
EE	768	9	0.051±0.0023	**0.032±0.001**	**0.95±0.27**	1.28±0.40
CAR	804	18	0.099±0.0028	**0.085±0.037**	**5180401± 808978.6**	5386755±807016.7
QSAR	908	7	0.12±0.001	0.08±0.001	**0.75±0.12**	0.76±0.12
CCS	1030	9	1.18±0.13	**0.13±0.038**	**23.73±1.18**	28.09±4.02
SOC	1056	6	0.07±0.01	**0.048±0.006**	**523.30±196.45**	579.31±202.70
GOM	1059	117	1.85±0.09	**1.56±0.077**	**244±26.31**	247.17±27.44
SF	1066	11	0.11±0.0044	**0.09±0.005**	0.67±0.2	0.67±0.19
ASN	1503	6	0.12±0.003	**0.08±0.001**	**9.6±1.1**	12.86±1.29
WINER	1599	12	0.40±0.051	**0.30±0.03**	**0.327±0.033**	0.329±0.03
AUV	2043	8	0.21±0.15	**0.15±0.008**	**6148974±770884.2**	9451554±952651.6
SG	3107	7	1.05±0.1	**0.92±0.082**	0.014±0.0047	0.014±0.0047
ABA	4177	9	1.60±0.15	**1.28±0.13**	**4.56±0.54**	4.59±0.55
WINEW	4898	12	**2.40±0.19**	2.49±0.50	0.364±0.021	0.364±0.019
CPU	8192	22	**9.77±0.47**	16.63±1.09	**5.79±0.53**	5.95±0.69
KRA	8192	9	**4.42±0.51**	6.22±1.05	0.0215±0.0006	**0.0214±0.0006**
PUMA	8192	33	**12.19±1.37**	14.24±4.15	0.0005±1.34e-5	0.0005±1.34e-5
GS	10000	13	**8.45±0.21**	16.81±2.18	**1.47e-4±3.39e-6**	1.5e-4±4.87e-6
BH	10692	10	**12.40±0.36**	22.47±0.39	**0.010±0.011**	0.011±0.011
NPP	11934	15	**12.62±1.09**	20.44±1.14	6.85e-7±9.48e-8	**6.54e-7±9.05e-8**
MH	13932	16	**15.51±0.55**	36.24±3.72	**0.021±0.001**	0.022±0.001
FIFA	19178	29	**43.63±5.05**	226.64±70.83	**0.57±0.024**	0.58±0.023
SUC	20263	82	**151.14±18.22**	216.39±166.09	85.19±5.99	**83.96±5.82**
CH	20460	9	**50.56±8.49**	108.80±20.00	**0.058±0.002**	0.059±0.002
KC	21613	22	**114.52±10.46**	447.15±99.89	**0.036±0.001**	0.037±0.001
HI	22272	12	**209.71±45.43**	326.13±78.25	215.79±4.51	**212.65±4.40**
CPS	28155	7	**28.55±7.36**	39.83±6.72	**0.27±0.0036**	0.28±0.0036
PP	45730	10	**311.77±48.19**	1439.81±142.50	12.27±0.18	**12.04±0.17**
SA	48933	22	**462.79±120.89**	2349.63±950.86	6.43±0.32	**6.33±0.32**

Table S6 : Training time of RLF and RF under simulated data

Sample size	Training time of RLF(seconds)	Training time of RF(seconds)
1000	0.29	0.20
10000	8.9	6.07
20000	26.51	123.98
30000	64.24	371.71
40000	90.72	829.43
50000	222.75	1649.24
60000	298.40	2583.99
70000	536.60	5050.07
80000	939.77	7141.25
90000	1499.06	9714.01

Simulated data are generated by the following regression model :

$$Y = 10 \cdot \prod_{j=1}^{10} e^{-2X_j^2} + \varepsilon, \quad \varepsilon \sim N(0, \sigma^2)$$

where $\mathbf{X}_j$ is the j-th dimension of an observation $\mathbf{X}$. Random sample X will be i.i.d and uniformly distributed on the 10-dimension unit discrete cube $[1, 2, 3, ..., 500]^{10}$ and $\sigma = 1$

F Proof of Theorem 3.1

For simplicity, we assume one-dimension case, i.e $Y = f(X)+\varepsilon$. Let A_1, A_2 be a nontrivial partition (mutually exclusive) of the initial outcome space, by the law of total variance or variance decomposition formula, we have

$$\begin{aligned} Var(Y) &= Var(Y(\mathbf{1}_{A_1} + \mathbf{1}_{A_2})) = Var(Y\mathbf{1}_{A_1}) + Var(Y\mathbf{1}_{A_2}) + 2Cov(Y\mathbf{1}_{A_1}, Y\mathbf{1}_{A_2}) \\ &= Var(Y|A_1)P(A_1) + Var(Y|A_2)P(A_2) + 2\left(E[Y^2\mathbf{1}_{A_1}\mathbf{1}_{A_2}] - E[Y\mathbf{1}_{A_1}] \cdot E[Y\mathbf{1}_{A_2}]\right) \end{aligned}$$

where $\mathbf{1}_{A_1}, \mathbf{1}_{A_2}$ are indicator functions for events A_1 and A_2, respectively.

Note that A_1 and A_2 are mutually exclusive, $\mathbf{1}_{A_1} \cdot \mathbf{1}_{A_2} = 0$. It follows that

$$\begin{aligned} Var(Y) &= Var(Y|A_1)P(A_1) + Var(Y|A_2)P(A_2) - 2E[Y\mathbf{1}_{A_1}]E[Y\mathbf{1}_{A_2}] \\ &= Var(Y|A_1)P(A_1) + Var(Y|A_2)P(A_2) - 2E[Y\mathbf{1}_{A_1}] \cdot (\mu - E[Y\mathbf{1}_{A_1}]) \end{aligned}$$

WLOG, we can assume $E[Y] = \mu = 0$, then we have

$$Var(Y) - Var(Y|A_1)P(A_1) - Var(Y|A_2)P(A_2) = 2(E[Y\mathbf{1}_{A_1}])^2$$

In Lebesgue cutting, we have $A_1 = \{Y \geq a\}, A_2 = \{Y < a\}$. Then the theoretical variance reduction of Y in the initial outcome space can be written as following:

$$Var(Y) - Var(Y|A_1)P(A_1) - Var(Y|A_2)P(A_2) = 2(E[Y\mathbf{1}_{Y>a}])^2$$

To find optimal splitting point a which gives the maximal variance reduction, we should solve the following optimization problem.

$$\max_a [L(a)]$$

where

$$L(a) = 2(E[Y\mathbf{1}_{Y\geq a}])^2$$

Similar argument applies for Riemann cutting. Let Riemann partition be $B_1 = \{X \geq b\}, B_2 = \{X < b\}$, then the corresponding optimization problem for Riemann cutting would be

$$\max_b \left[2(E[Y\mathbf{1}_{X>b}])^2\right] = \max_b [R(b)]$$

where

$$R(b) = 2(E[Y\mathbf{1}_{X\geq b}])^2$$

Consider the optimal Riemann splitting b^* which achieves the maximum of $R(b)$,i.e. $R(b^*) \geq R(b)$, for any b in the domain of X. Denote $a^* = E[Y\mathbf{1}_{X\geq b^*}]$ and we have $a^* \leq E[Y] = 0$. Thus the probability of event $Y \geq a^*$ is positive as $EY = 0$. Since $Y\mathbf{1}_{Y\geq a^*} \geq a^*$, we have

$$E[Y\mathbf{1}_{Y\geq a^*}] \geq a^* = E[Y\mathbf{1}_{X\geq b^*}]$$

It follows that

$$\max_a[L(a)] \geq 2(E[Y\mathbf{1}_{Y>a^*}])^2 \geq 2(E[Y\mathbf{1}_{X>b^*}])^2 = \max_b[R(b)] \tag{10}$$

In other words, the optimal Lebesgue cutting can reduce at least the same variance as optimal Riemann cutting (CART) does. We can also see the noise doesn't affect the conclusion since Y already absorbed noises in practice.

Another analysis of equation 10 from discrete case:

In discrete case, we need to compare $L(j^*, s^*)$ and $\tilde{L}(s_L^*)$ as defined in equation 4 and equation 5.

Note that the set of possible partitions of current set of responses induced by the Riemann cutting of covariate $\mathbf{X}$ is a subset of that of Lebesgue cutting whose feasible set is essentially induced by response directly. Note that the objective functions $L(j, s)$ and $\tilde{L}(s)$ have the same form, the one with larger feasible set should have larger optimal value.

Suppose we have n points $\{(X_1, Y_1), ..., (X_n, Y_n)\}$ whose y values are all distinct in a certain non-terminal node and both cutting types employ CART split criterion, then Lebesgue cutting will go through all $(n+1)$ splitting points in Y directly, which essentially gives the largest feasible set of optimization problem. On the other hand, in Riemann type cutting, the space of Y is indirectly partitioned by going through all possible splitting points in direction $X^{(j)}$. It's not necessary that this procedure will take care all $(n+1)$ splitting points in Y. For example, when $X^{(j)}$ is a direction with only three distinct values , $z^{(j)}$ can only have four choices of splitting point which will restrict the possible values of $\bar{Y}_{A_L}, \bar{Y}_{A_R}$ in optimizing $L(j, s)$ and leads to a smaller feasible set.

G Proof of Theorem 3.2

We basically follows the idea in (Peng et al., 2019) which decomposes the generalized incomplete U-statistic as a sum of complete U-statistic and a remainder. To deal with the random kernel, we utilize the conclusions based on extended Hoeffding decomposition (Peng et al., 2019). For the simplicity of notation, it's harmless to assume that $\theta = 0$.

For $0 < \eta_0 < \frac{1}{2}$, we first decompose $U_{n,k,N,\omega}/\sqrt{k^2\zeta_{1,\omega}/n + \zeta_k/N^{2\eta_0}}$ as follows:

$$\begin{aligned}\frac{U_{n,k,N,\omega}}{\sqrt{\frac{k^2\zeta_{1,\omega}}{n} + \frac{\zeta_k}{N}}} &= \frac{\frac{1}{\binom{n}{k}}\sum_{(n,k)}\frac{\rho_i}{p}h^{(\omega_i)}(Z_{i_1}, ..., Z_{i_k}) + \frac{1}{\binom{n}{k}}\sum_{(n,k)}\frac{W_i-\rho_i}{p}h^{(\omega_i)}(Z_{i_1}, ..., Z_{i_k})}{\sqrt{\frac{k^2\zeta_{1,\omega}}{n} + \frac{\zeta_k}{N}}} \\ &= \frac{A + \frac{1}{\binom{n}{k}}\sum_{(n,k)}\frac{W_i-\rho_i}{p}h^{(\omega_i)}(Z_{i_1}, ..., Z_{i_k})}{\sqrt{\frac{k^2\zeta_{1,\omega}}{n} + \frac{\zeta_k}{N}}}\end{aligned} \tag{11}$$

where

$$\begin{aligned}A &= \frac{1}{\binom{n}{k}}\sum_{(n,k)}\frac{\rho_i}{p}h^{(\omega_i)}(Z_{i_1}, ..., Z_{i_k}) \\ &= \frac{\hat{N}}{N}\frac{1}{\hat{N}}\sum_{(n,k)}\rho_i h^{(\omega_i)}(Z_{i_1}, ..., Z_{i_k})\end{aligned} \tag{12}$$

and $\rho_i \overset{i.i.d}{\sim} Bernoulli(p)$, $p = N/\binom{n}{k}$ and $\hat{N} = \sum_{(n,k)}\rho_i$. We can see $E[\hat{N}] = N$. WLOG, we can assume $\theta_{n,k,N} = 0$. Then we have

$$A = \frac{\hat{N}}{N}B \tag{13}$$

where

$$B = \frac{1}{\hat{N}}\sum_{(n,k)}\rho_i h^{(\omega_i)}(Z_{i_1}, ..., Z_{i_k})$$

and B is a complete generalized U-statistic with Bernoulli sampling as described in (Peng et al., 2019). According to Theorem 4 in Peng et al. (2019), we have

$$
\begin{aligned}
sup_{z\in R}\left|P\left(\frac{B}{\sqrt{k^2\zeta_{1,\omega}/n+\zeta_k/N}}\right)-\Phi(z)\right| &\leq C\Bigg\{\frac{\mathbb{E}|g|^3}{n^{1/2}\zeta_{1,\omega}^{3/2}}+\frac{\mathbb{E}|h|^3}{N^{1/2}(\mathbb{E}|h|^2)^{3/2}} \\
&\quad +\left[\frac{k}{n}\left(\frac{\zeta_k}{k\zeta_{1,\omega}}-1\right)\right]^{1/2}+\left(\frac{k}{n}\right)^{1/3}+N^{-\frac{1}{2}+\eta_0}\Bigg\} \\
&:= \varepsilon_0
\end{aligned}
\tag{14}
$$

where $0<\eta_0<1/2$.

By definition, we have $\zeta_k = var(h) = \mathbb{E}|h|^2 = \Sigma^2_{k,n,\omega,\mathbf{Z}}$

Denote

$$
T=\frac{A}{\sqrt{k^2\zeta_{1,\omega}/n+\zeta_k/N}}=W+\Delta
$$

where

$$
W=\frac{B}{\sqrt{k^2\zeta_{1,\omega}/n+\zeta_k/N}},\quad \Delta=(\frac{\hat{N}}{N}-1)W
$$

According to the argument in proof of Theorem 4 in (Peng et al., 2019), it's easy to verify that

$$
-P\Big(z-|\Delta|\leq W\leq z\Big)\leq P\Big(U\leq z\Big)-P\Big(W\leq z\Big)\leq P\Big(z\leq W\leq z+|\Delta|\Big)
$$

Thus we only need to consider bounding $P(z\leq W\leq Z+|\Delta|)$. By Bernstein's inequality, we have

$$
P\left(|\frac{\hat{N}}{N}-1|\geq\varepsilon\right)\leq 2exp\left(-\frac{-\varepsilon^2N}{1-p+\varepsilon/3}\right)
$$

Let $\varepsilon=N^{-\beta}$ and note that $P(|Z|\geq N^{\alpha})\leq 2exp(-N^{2\alpha}/2)$, we have

$$
\begin{aligned}
P(|\Delta|\geq N^{-\beta+\alpha}) &\leq P\left(|\frac{\hat{N}}{N}-1|\geq N^{-\beta}\right)+P(|W|\geq N^{\alpha}) \\
&\leq 2\exp\left(-\frac{N^{1-2\beta}}{1-p+N^{-\beta}/3}\right)+P(|Z|\geq N^{\alpha})+2\varepsilon_0 \\
&\leq 2\exp\left(-\frac{1}{(1-p)N^{2\beta-1}+N^{\beta-1}/3}\right)+2\exp(-N^{2\alpha/2})+2\varepsilon_0 \\
&:= \varepsilon_1+2\varepsilon_0
\end{aligned}
\tag{15}
$$

Eventually, we can bound $P(z\leq W\leq z+|\Delta|)$ as follows:

$$
\begin{aligned}
P(z\leq W\leq z+|\Delta|) &\leq P(z\leq W\leq z+|\Delta|,|\Delta|\leq N^{-\beta+\alpha})+P(|\Delta|\geq N^{-\beta+\alpha}) \\
&\leq P(z\leq W\leq z+N^{-\beta+\alpha})+\varepsilon_1+2\varepsilon_0 \\
&\leq 2\varepsilon_0+P(z\leq Z\leq z+N^{-\beta+\alpha})+\varepsilon_1+2\varepsilon_0 \\
&\leq 4\varepsilon_0+\varepsilon_1+\frac{1}{\sqrt{2\pi}}N^{-\beta+\alpha} \\
&:= 4\varepsilon_0+\varepsilon_1+\varepsilon_2
\end{aligned}
\tag{16}
$$

Let $\beta=0.5+\eta_1$ and $\alpha=\eta_1$, where $\eta_1>0$. It's easy to see $\varepsilon_1\ll\varepsilon_2$ when N is large and therefore

$$
\begin{aligned}
\sup_{z\in R}\left|P\left(\frac{A}{\sqrt{k^2\zeta_{1,\omega}/n+\zeta_k/N}}\right)-\Phi(z)\right| &= \sup_{z\in R}\left|P(T\le z)-\Phi(z)\right| \\
&\le \sup_{z\in R}\left|P(W\le z)-\Phi(z)\right| + \sup_{z\in R}\left|P(T\le z)-P(W\le z)\right| \\
&\le 5\varepsilon_0+\varepsilon_1+\varepsilon_2 \\
&= C\Bigg\{\frac{\mathbb{E}|g|^3}{n^{1/2}\zeta_{1,\omega}^{3/2}}+\frac{\mathbb{E}|h|^3}{N^{1/2}(\mathbb{E}|h|^2)^{3/2}} \\
&+\left[\frac{k}{n}\left(\frac{\zeta_k}{k\zeta_{1,\omega}}-1\right)\right]^{1/2}+\left(\frac{k}{n}\right)^{1/3}+N^{-\frac{1}{2}+\eta_0}+N^{-\frac{1}{2}}\Bigg\} \\
&:= \varepsilon_3
\end{aligned}
\tag{17}
$$

We observe that the factor of $\hat{N}/N$ only produces the extra term $N^{-\frac{1}{2}}$ in the final bound, which is similar to (Peng et al., 2019). We employ this technique one more time to achieve the bound for $U_{n,k,N,\omega}$.

Denote

$$
\frac{U_{n,k,N,\omega}}{\sqrt{\frac{k^2\zeta_{1,\omega}}{n}+\frac{\zeta_k}{N}}}=\frac{A}{\sqrt{\frac{k^2\zeta_{1,\omega}}{n}+\frac{\zeta_k}{N}}}+C=\frac{A}{\sqrt{\frac{k^2\zeta_{1,\omega}}{n}+\frac{\zeta_k}{N}}}+\frac{D}{\sqrt{k^2\zeta_{1,\omega}/n+\zeta_k/N}}
$$

where A is defined as above and

$$
C=\frac{\frac{1}{\binom{n}{k}}\sum_{(n,k)}\frac{W_i-\rho_i}{p}h^{(\omega_i)}(Z_{i_1},...,Z_{i_k})}{\sqrt{k^2\zeta_{1,\omega}/n+\zeta_k/N}},\quad D=\frac{1}{\binom{n}{k}}\sum_{(n,k)}\frac{W_i-\rho_i}{p}h^{(\omega_i)}(Z_{i_1},...,Z_{i_k})
$$

Again, we only need to bound $P\left(z\le\frac{A}{\sqrt{\frac{k^2\zeta_{1,\omega}}{n}+\frac{\zeta_k}{N}}}\le z+|C|\right)$. Let $0<\eta_0<\frac{1}{2}$, by Jensen's inequality, we have

$$
\begin{aligned}
P(|C|\ge N^{\eta_0-1/2}) &\le N^{\frac{1}{2}-\eta_0}\mathbb{E}[|C|] \\
&\le N^{\frac{1}{2}-\eta_0}\sqrt{\mathbb{E}[|C|^2]}
\end{aligned}
\tag{18}
$$

Note that Ghosal & Hooker (2021) illustrates that these two selection schemes (sampling without replacement and Bernoulli sampling) are asymptotically the same. More specifically, one can show that

$$
\mathbb{E}[|D|^2]=\mathbb{E}\left[\left(\frac{1}{N}\sum_i(W_i-\rho_i)h^{(\omega_i)}(\mathbf{Z}_i)\right)^2\right]=K\left[\frac{1}{N}-\frac{1}{\binom{n}{k}}\right]
$$

where $\mathbf{Z}_i$ represents the i-th subsample from $\mathbf{Z}=(Z_1,...,Z_n)$ and $K=\mathbb{E}[(h^{(\omega_i)}(\mathbf{Z}_i))^2]=Var(h^{(\omega_i)}(\mathbf{Z}_i))=\zeta_k$ since we assume that $\theta=0$.

It follows that

$$
\begin{aligned}
P(|C| \geq N^{\eta_0 - 1/2}) &\leq N^{\frac{1}{2}-\eta_0} \left(K(\frac{1}{N} - \frac{1}{\binom{n}{k}}) \right)^{\frac{1}{2}} \left(\frac{k^2 \zeta_{1,\omega}}{n} + \frac{\zeta_k}{N} \right)^{-\frac{1}{2}} \\
&= (K(1-p))^{\frac{1}{2}} \left(\frac{N^{2\eta_0} k^2 \zeta_{1,\omega}}{n} + \frac{N^{2\eta_0} \zeta_k}{N} \right)^{-\frac{1}{2}} \\
&= (K(1-p))^{\frac{1}{2}} \left(\frac{k^2 \zeta_{1,\omega}}{n/N^{2\eta_0}} + N^{2\eta_0 - 1} \zeta_k \right)^{-\frac{1}{2}} \\
&\leq (K(1-p))^{\frac{1}{2}} \left(\frac{k^2 \zeta_{1,\omega}}{n/N^{2\eta_0}} \right)^{-\frac{1}{2}} \\
&= (K(1-p))^{\frac{1}{2}} \left(\frac{n/N^{2\eta_0}}{k^2 \zeta_{1,\omega}} \right)^{\frac{1}{2}} \\
&= \left(\frac{n}{N^{2\eta_0}} \frac{(1-p)\zeta_k}{k^2 \zeta_{1,\omega}} \right)^{\frac{1}{2}}
\end{aligned}
\tag{19}
$$

Eventually, we can bound $P\left(z \leq \frac{A}{\sqrt{\frac{k^2\zeta_{1,\omega}}{n} + \frac{\zeta_k}{N}}} \leq z + |C| \right)$ as follows:

$$
\begin{aligned}
P\left(z \leq \frac{A}{\sqrt{\frac{k^2\zeta_{1,\omega}}{n} + \frac{\zeta_k}{N}}} \leq z + |C| \right) &\leq P\left(z \leq \frac{A}{\sqrt{\frac{k^2\zeta_{1,\omega}}{n} + \frac{\zeta_k}{N}}} \leq z + |C|, |C| \leq N^{-1/2} \right) + P(|C| \geq N^{-1/2}) \\
&\leq P\left(z \leq \frac{A}{\sqrt{\frac{k^2\zeta_{1,\omega}}{n} + \frac{\zeta_k}{N}}} \leq z + N^{-1/2} \right) + \left(\frac{n}{N^{2\eta_0}} \frac{(1-p)\zeta_k}{k^2 \zeta_{1,\omega}} \right)^{\frac{1}{2}} \\
&\leq \varepsilon_3 + P(z \leq Z \leq z + N^{-1/2}) + \left(\frac{n}{N^{2\eta_0}} \frac{(1-p)\zeta_k}{k^2 \zeta_{1,\omega}} \right)^{\frac{1}{2}} \\
&\leq \varepsilon_3 + \frac{1}{\sqrt{2\pi}} N^{-1/2} + \left(\frac{n}{N^{2\eta_0}} \frac{(1-p)\zeta_k}{k^2 \zeta_{1,\omega}} \right)^{\frac{1}{2}}
\end{aligned}
\tag{20}
$$

Note that ε_3 also includes terms of order $N^{-1/2}$ and therefore

$$
\begin{aligned}
\sup_{z \in R} \left| P\left(\frac{U_{n,k,N,\omega}}{\sqrt{k^2\zeta_{1,\omega}/n + \zeta_k/N}} \right) - \Phi(z) \right| &\leq \sup_{z \in R} \left| P(\frac{A}{\sqrt{\frac{k^2\zeta_{1,\omega}}{n} + \frac{\zeta_k}{N}}} \leq z) - \Phi(z) \right| \\
&\quad + \sup_{z \in R} \left| P(U_{n,k,N,\omega} \leq z) - P(\frac{A}{\sqrt{\frac{k^2\zeta_{1,\omega}}{n} + \frac{\zeta_k}{N}}} \leq z) \right| \\
&\leq \varepsilon_3 + \varepsilon_3 + \frac{1}{\sqrt{2\pi}} N^{-1/2} + \left[\frac{n}{N^{2\eta_0}} \frac{(1-p)\zeta_k}{k^2 \zeta_{1,\omega}} \right]^{\frac{1}{2}} \\
&= \tilde{C} \Bigg\{ \frac{\mathbb{E}|g|^3}{n^{1/2} \zeta_{1,\omega}^{3/2}} + \frac{\mathbb{E}|h|^3}{N^{1/2} (\mathbb{E}|h|^2)^{3/2}} \\
&\quad + \left[\frac{k}{n} \left(\frac{\zeta_k}{k\zeta_{1,\omega}} - 1 \right) \right]^{1/2} + \left(\frac{k}{n} \right)^{1/3} + N^{-\frac{1}{2}+\eta_0} \\
&\quad + \left[\frac{n}{N^{2\eta_0}} \frac{(1-p)\zeta_k}{k^2 \zeta_{1,\omega}} \right]^{\frac{1}{2}} \Bigg\}
\end{aligned}
\tag{21}
$$

where $\tilde{C}$ is a positive constant.

H Tuning results for two examples

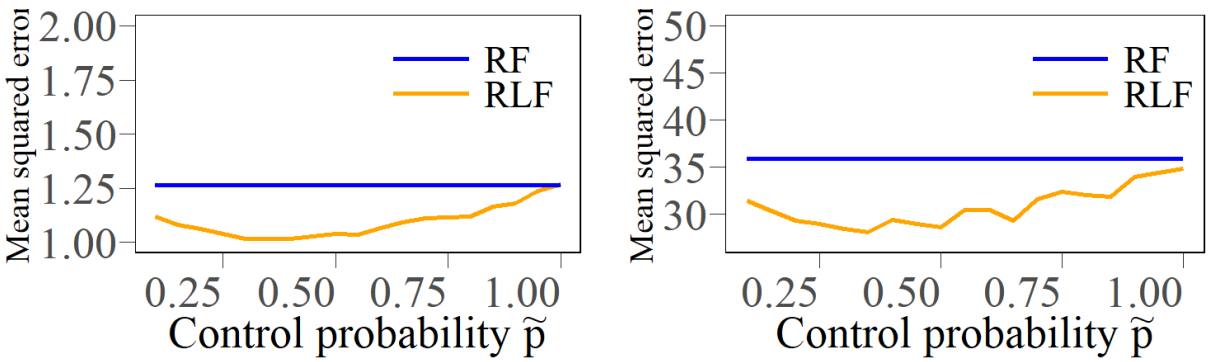

(a) Example 1

(b) Example 2

Figure S4: Test MSE curve as function of control probability $\tilde{p}$ in two examples

Table S7 : Top 10 tuned models for RLF and RF for Example 1

Rank of Validation MSE	RF	α	M_{node}	M	RLF	$\tilde{p}$	M_{local}
1	1.308092	0.5	15	100	1.081210	0.4	10
2	1.309780	0.5	5	50	1.085926	0.4	20
3	1.313989	0.5	15	200	1.088091	0.4	50
4	1.315487	0.63	5	200	1.117446	0.6	50
5	1.316665	0.5	5	100	1.125599	0.6	10
6	1.316748	0.63	10	50	1.127653	0.6	20
7	1.320919	0.8	10	200	1.128331	0.2	10
8	1.326341	0.5	10	50	1.150248	0.2	20
9	1.327373	0.8	5	150	1.164717	0.2	50
10	1.327539	0.63	10	150	1.197099	0.8	20

Table S8 : Testing MSE under optimal model for Example 1:

	Bset RF	Best RLF
Testing MSE	1.283	1.018

Table S9 : Top 10 tuned models for RLF and RF for Example 2

Rank of Validation MSE	RF	α	M_{node}	M	RLF	$\tilde{p}$	M_{local}
1	33.18551	0.63	15	100	28.48683	0.4	10
2	34.40944	0.5	15	50	29.34517	0.2	10
3	34.53584	0.63	5	200	29.53972	0.4	20
4	34.61853	0.63	10	100	29.72733	0.4	50
5	34.64231	0.63	5	50	29.98644	0.2	20
6	34.76124	0.8	5	50	30.22297	0.6	10
7	34.78667	0.63	10	150	30.31668	0.2	50
8	34.84602	0.5	15	150	30.33824	0.6	50
9	34.99652	0.8	5	150	30.94450	0.6	20
10	35.19693	0.63	15	150	32.03192	0.8	10

Table S10 : Testing MSE under optimal model for Example 2:

	Best RF	Best RLF
Testing MSE	35.17	29.87

Tuning procedure: For each example, we generated 3000 samples from the corresponding model and divide in into three parts for training, validation and testing. The ratio is 6:2:2. For RF, we set subagging ratio $\alpha \in \{0.5, 0.63, 0.8\}$, minimal node size $M_{node} \in \{5, 10, 15\}$ and number of trees $M \in \{50, 100, 150, 200\}$. For RLF, we keep $M = 100$ and $\alpha = 0.63$ all the time for efficiency. We set $\tilde{p} \in \{0.2, 0.4, 0.6, 0.8\}$ and $M_{local} \in \{10, 20, 50\}$ which are two new parameters introduced in RLF. Fig. S4(a) and S4(b) are Test MSEs for RLF as functions of $\tilde{p}$ with $M = 100, M_{local} = 10$. For RF, we use the default setting.

I Extra experiments with tuned RLF and RF

We performed extra experiments on 26 datasets (due to the time efficiency of parameter tuning) to compare best RF and best RLF.

We performed 5-fold cross validations to ensure 20% of observations are used as testing set. For the rest of 80% points, we further randomly pick 25% of them as validation set, which is used to select best models among parameter space. As a result, the ratio of training,validation and testing is 6:2:2.

Tuning parameters for RLF: $\tilde{p} \in \{0.4, 0.6, 0.8\}$. We set $M = 100, M_{local} = 10, M_{node} = 5$ all the time for RLF due to the time efficiency. Tuning parameters for RF: $M \in \{50, 150, 200\}, M_{node} \in \{5, 10, 15\}$. Other parameters for RLF and RF follow the default value. Note that the implementation of RF in R doesn't have parameter of tree depth but we can control and depth of tree by the value of minimal size of node M_{node}.

J Extra experiments: Ablation study with feature selection

Table S11 : Testing MSE for ablation study(10-fold cross-validation)

Dataset	RLF+feature selection	RF+feature selection	RLF(100,10)
FF	4246.598 ± 5488.292	4255.631 ±5497.251	**4205.21 ±5612.77**
SP	**1.60 ±0.62**	1.72± 0.62	1.90±0.87
CARS	18396078 ± 2977821	20540942± 3358102	**5374313±787019.9**
ABA	7.24 ± 0.68	7.26± 0.67	**4.63 ±0.54**
KRA	0.05 ± 0.0018	0.051± 0.0019	**0.0188 ±0.00062**
NPP	6.77e-6 ± 4.0e-75	1.92e-5± 9.58e-7	**5.97e-7±6.84e-8**
GOM	**234.149 ± 26.31**	236.12± 28.65	240.67±38.74
SF	**0.6178 ± 0.224**	0.6183± 0.225	0.66±0.21
CCS	79.86 ± 7.21	82.36± 7.38	**28.34±4.87**
SOC	618.86 ± 180.31	635.35± 175.40	**587.87±205.53**
EE	4.25 ± 0.87	6.00± 0.95	**1.258±0.32**
QSAR	0.97 ± 0.15	0.98± 0.15	**0.7568 ±0.14**
ASN	28.02 ± 2.31	28.07± 2.28	**11.87 ±1.28**
WINER	0.35 ± 0.032	0.34± 0.033	**0.3319±0.034**
AUV	14457235± 2492794	17803133±2024322	**8073182 ±1513348**
SG	0.0183 ± 0.005	0.0182± 0.005	**0.01367 ±0.0045**
WINEW	0.41 ± 0.018	0.42± 0.018	**0.367±0.021**
CPU	249.68± 21.71	251.67± 23.39	**5.72 ±0.63**
PUMA	**0.000495± 1.17e-5**	0.0005± 1.24e-5	4.97e-4±1.38e-5
GS	0.00074± 2.10e-5	0.00075± 2.13E-5	**1.2e-4±4.06e-6**
BH	0.0127± 0.00961	0.0142± 0.010	**0.01 ±0.01**
MH	0.041± 0.0023	0.045± 0.0022	**0.02 ±0.0009**
FIFA	0.588± 0.023	0.593 ± 0.024	**0.5775±0.026**

Table S12 : Testing MSE for sparse model ablation study(10-fold cross-validation)

	RF+feature selection	RLF+feature selection	RLF
Testing MSE	3.90 ± 0.35	**3.78 ± 0.33**	4.17 ± 0.40

K Extra experiments: Missing value case

Table S13 : Testing MSE(10-fold cross-validation) of RLF and RF under missing value cases

Dataset	RLF	RF
Moneyball	**656.91 ± 84.90**	670.11 ± 94.46
FPSbenchmark	**11.04 ± 0.55**	20.24± 0.95